Quantitative EEG in Predicting Coma Outcome

Sabina Stefan[1]

[1]Bioinformatics, University of Cape Town, South Africa

Supervisor: Dr Shock

Abstract

Motivation: Currently, the manner in which EEG data is used in clinical practice to prognosticate coma may be unsophisticated, subjective and prone to human error, which has potentially serious consequences in end-of-life decision making. A quantitative, statistically-based approach to EEG data analysis of comatose patients may reveal prognostic markers that would otherwise escape detection.

Results: We extracted several descriptive parameters from resting-state EEG data of UWS and MCS patients (n=58) using signal processing techniques and mathematical methods, and assessed the prognostic power of these parameters using the outcomes (positive or negative) of these patients 12 months after EEG recording. We additionally investigated the power of these measures in discriminating UWS/MCS patients, considering that in clinical practice diagnosis is often used to inform prognosis. Lastly, we aimed to develop an automatic system for coma outcome prediction by combining the 3 best-performing features in a single classification scheme.

The features considered here were drawn from five main categories: microstate analyses, entropy, frequency power analyses, connectivity and complex network analyses. Of these measures, we found that the best results at predicting outcome were obtained by the clustering coefficient of EEG signals represented as complex network graphs calculated from thresholding beta coherence (AUC = 88% $\pm$ 3%). The characteristic path length of these complex network graphs determined from alpha coherence most reliably indexed the consciousness of UWS and MCS patients (AUC = 78% $\pm$ 3%). Several other measures exhibited significant predictive and/or discriminatory power, indicating promise in a quantitative approach. We furthermore found that the automatic classification system afforded accurate results (AUC = 95% $\pm$ 2%), and thus may contribute to accurate prognosis in clinical practice. A toolbox for qEEG analyses is also made available in both Python and MATLAB at: https://qeeg.wordpress.com

Abbreviations: ApEn = Approximate Entropy, AUC = area under the curve, MCS = minimally conscious state, UWS = unresponsive wakefulness syndrome

1 Introduction

Coma is a dynamic state of unconsciousness with a multitude of aetiologies, all of which include injury or malfunction of the cerebral cortex or reticular activating system or both (Plum and Posner, 1982). Patients may recover well from coma, while others may remain in an Unresponsiveness Wakefulness Syndrome (UWS), characterised by wakefulness without awareness (Laureys *et al.*, 2010), or a Minimally Conscious State (MCS), defined by definite but minimal awareness of oneself and one's environment (Giacino *et al.*, 2002). For ethical, therapeutic and economic reasons, it is important to predict coma outcome as reliably and sensitively as possible.

In current practice, the diagnosis and prognosis of coma are most often established using clinical methods, such as the examination of pupillary reflexes, and electroencephalography (EEG) techniques, which assess the electrical activity of the brain as recorded from multiple electrodes along the scalp (Bradley, 2004). Because EEG is a non-invasive, safe and relatively easy manner of gauging the function of the brain, considerable research has been done to develop methods to better understand and interpret these signals. Applied to coma, these methods are focussed on the objective assessment of EEG signals and aim to detect subtlety that may escape visual inspection, thus minimising subjectivity and human error in the prognostication of coma. Moreover, these methods aim to challenge the manner in which EEG is currently used in clinical practice by providing a rigorous, objective and statistically-based analysis of the data, typically through the mathematical extraction of descriptive parameters. In this study, we investigate a quantitative approach to EEG analyses in coma outcome prediction by applying principles from mathematical disciplines like nonlinear dynamics and chaos as well as graph theory to the study of EEG signals of comatose patients. Some of the methods employed here, like microstate analyses, have been successful in other EEG studies in ascertaining truths about conditions like schizophrenia and narcolepsy (Lehmann *et al.*, 2005, Kuhn *et al.*, 2014) and we therefore examine whether these methods additionally provide insights on the brain function of comatose patients. Other methods investigated here are motivated by theoretical considerations: it is believed that disorders of consciousness may stem from a disruption in the functional connection, communication and information-sharing between different cortical networks (Laureys *et al.*, 2000, 1999). Measures like connectivity, entropy and graph-theoretical statistics aim to interrogate these theoretical claims.

In this study, we aim to investigate the power of numerous measures as biomarkers in predicting positive and negative outcomes of coma, where outcomes are defined by the survival state of the patient 12 months after having recorded the EEG. Furthermore, we investigate the power of these measures in discriminating between UWS and MCS patients, considering that diagnosis (UWS or MCS) may often play a crucial role in prognosis (Giacino, 2004), despite the wide prevalence of misdiagnoses (van Erp *et al.*, 2015a). For this reason, it may be useful to determine potential biomarkers of consciousness that assist in diagnosis as they thereby may assist in prognosis.

Lastly, we predict the outcome of patients using a combination of the 3 best-performing features, with the intention of investigating the possibility of automatic outcome prediction in clinical practice. An automatic system based on EEG has a number of benefits: the technology is easy and cost-effective to implement, it completely avoids subjective analysis and requires little or no medical expertise.

2 Data and materials

2.1 Data

For all quantitative EEG analyses, data was obtained from the HOPE project (Lopez-Rolon *et al.*, 2015). This data consists of resting-state data sampled at 1000Hz collected from 256 channels positioned according to the International 10-20 system. This data is segmented into artifact-free epochs of 2s and passed through a high-pass filter of 1Hz to eliminate slow drifts.

2.2 Statistical analyses

To determine the predictive power of the measures explored in this study, patients were classified into binary groups by fitting a generalised linear model on training data, and testing the model on test data. Additionally, to avoid over-fitting and circular analysis, a ten-fold stratified cross-validation scheme was implemented. The performance of the classifiers was then investigated using receiver operating characteristic (ROC) curves. The ROC curve is a graphical plot that illustrates the performance of a binary classifier by plotting the true positive rate (sensitivity) against the false positive rate (1-specificity) at various thresholds. If the value of a feature of a patient is greater than a certain threshold, the patient is classified into a group, or otherwise classified into the other group.

We calculated the area under the curve (AUC) of ROC curves to determine which features exhibited significant differences across groups of patients. The area under the curve (AUC) of a ROC provides a measure of classification accuracy, such that an AUC of 100% indicates perfect classification and 50% indicates random classification. Significance of AUC was established by randomly permuting the elements of feature vectors and comparing the results using non-parametric statistics (Mason and Graham, 2002).

Finally, to account for multiple comparisons, the false discovery rate was controlled by employing the Benjamini-Hochberg procedure at level $\alpha = 0.05$. The procedure is as follows: the p-values, $p_1 \dots p_m$, corresponding to the null hypotheses (features tested), $H_1, \dots H_m$, are ordered in increasing order. Each p-value is compared to the Benjamini-Hochberg critical value, $\frac{i}{m}\alpha$, where i is the rank and m is the number of hypotheses. The largest p-value that is less than the critical value is considered to be significant, as well as all p-values smaller than it. Adjusted p-values are calculated as raw p-values multiplied by $\frac{m}{i}$, and are reported in this study as q-values.

All analyses were performed using both MATLAB and Python, and some analyses required the use of facilities from the University of Cape Town's High Performance Computing centre.

3 Methods

3.1 Microstate Analysis

Microstate analysis is a spatio-temporal method that analyses the topographical maps of electric potentials over the electrode array as well as the temporal evolution of these topographies, such that multi-channel EEG data is essentially considered as a series of sequential topographies of electric fields (Pascual-Marqui *et al.*, 1995). Interestingly, most studies find that four archetypal maps account for over 70% of total topographical variance, and furthermore that EEG topography remains quasi-stable for about 80-120ms before abruptly changing into a topography represented by a different archetypal map (Murray *et al.*, 2008). Microstates are thus defined as these archetypal maps of quasi-stability, during which global topography is invariant, although electric field strength may vary and polarity invert (Lehmann *et al.*, 1987). It has been suggested that microstates reflect primitive information processing as the most basic initializations of neurological tasks (Lehmann *et al.*, 1998).

Microstate analyses have proven to be useful in differentiating people with different brain states. For example, it has been shown that one microstate class in schizophrenics displayed significantly different field configurations and shorter durations in patients than controls (Lehmann *et al.*, 2005). Furthermore, microstate analyses have been applied to investigate differences between narcoleptic patients and controls, to probe the brain in different sleeping stages, as well as to reflect personality differences between skeptics and believers in paranormal phenomena (Kuhn *et al.*, 2014, Brodbeck *et al.*, 2012, Schlegel *et al.*, 2012).

The microstate segmentation was performed similarly to other studies. Specifically, the EEG data was transformed to the average-reference, the Global Field Power (GFP) was calculated for each trial, and the topographic maps extracted at time points of GFP local maxima, which correspond to times of greatest signal-to-noise ratio (Koenig and Melie-García, 2010). The GFP is essentially the standard deviation of the voltages recorded at all channels at each time point, and can be calculated as,

$$\text{GFP} = \sqrt{\frac{\sum_{i=1}^{N}(u_i - \bar{u})^2}{N}} \tag{1}$$

where u_i is the voltage at electrode i, $\bar{u}$ is the average voltage of all electrodes, and N is the number of electrodes.

These maps at GFP maxima are assimilated for all trials, and clustered into a predetermined number of clusters using a modified k-means or a "Topographical Atomise and Agglomerate Hierarchial Clustering" algorithm (Murray *et al.*, 2008). Here, the data was analysed using both clustering methods to account for potential differences in the microstates obtained using the different clustering methods.

Microstates in the delta (0-4 Hz), theta (4-8 Hz), alpha (8-13 Hz), and 2-20 Hz frequency bands were obtained after having filtered data in the respective frequency bands using a second-order Butterworth filter. For each frequency band, the following outputs were obtained for each patient,

- EEG scalp topographies when data is segmented into four microstates.
- The average number of times a microstate appears in a trial of EEG data.
- The average duration of each microstate in a trial.
- The average percentage of time spent in each microstate.

To achieve this, firstly four global microstates were obtained by pooling all patient data and clustering topographies, as shown in Figure 1. For each patient, the topographies at GFP maxima were then compared with each global microstate by computing squared correlation coefficients so as to disregard polarity. Each topography was then assigned to a microstate class A, B, C or D dependent on the global microstate with which it best correlated, so that this process is much like a modified k-means clustering algorithm with the global maps as seed maps. The first spatial principal component was calculated for each microstate class to obtain four representative maps for each patient, which were then used in subsequent analyses.

For each patient, topographies at GFP maxima were compared to each microstate class by calculating squared correlation coefficients, and assigned to the class with which they best correlated. The average frequency, duration and percentage of time spent in each microstate were then determined, considering that EEG topographies remain stable between GFP minima as determined by previous research (Michel, 2009). This procedure is illustrated in Figure 2.

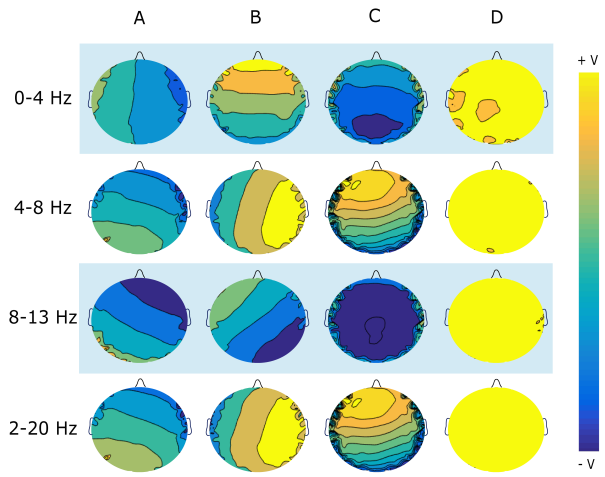

Fig. 1. Global microstate classes, A, B, C and D, obtained in the delta, theta, alpha and 0-20Hz frequency bands, which are essentially used as seep maps when determining microstate classes for each individual patient.

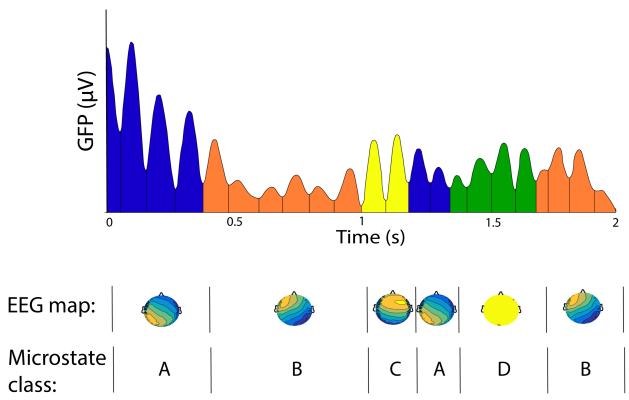

Fig. 2. The microstate analysis for one trial of data for one patient. Firstly, microstate classes, A, B, C and D, are obtained for each patient using a clustering algorithm, and then topographic maps at each time point are assigned to a microstate class. The different colours of the GFP curve represent the four microstate classes. The corresponding microstate topography at each time point, as well as the microstate class, are illustrated beneath the GFP curve.

3.2 Entropy

Measures of entropy aim to quantify the unpredictability of outputs of the complex system of neural networks underlying consciousness. Numerous measures of entropy have been applied to the analysis of EEG signals, particularly in the studies of anesthesia and epilepsy (Bruhn *et al.*, 2000, Kannathal *et al.*, 2005). However, measures of entropy, such as Approximate Entropy (ApEn) and permutation entropy specifically, are increasingly being investigated with relation to coma and consciousness, with some interesting preliminary results. For example, Sarà *et al.* have shown a correlation between ApEn measures and outcome of patients in the vegetative state (Sarà *et al.*, 2011), although Gosseries *et al.* found entropy to only be useful in diagnosis, and not prognosis (Gosseries *et al.*, 2011). The present study extends the work of previous studies in analysing ApEn as a predictor of coma outcome, and also investigates the prognostic value of permutation entropy as explored for the first time, as far as we know. These measures of entropy may be useful because they are scale-invariant, robust to noise, and discriminate series for which clear feature recognition is difficult (Pincus, 1995, Pincus and Goldberger, 1994).

Approximate Entropy

Conceptually, ApEN is defined as the logarithmic likelihood that the patterns of data that are close to each other will remain close on following incremental comparisons. Mathematically, ApEn is determined as follows:

Given a segment of EEG of N time samples, $[u(1), u(2), \ldots, u(N)]$, and an arbitrary value m, a sequence of vectors $[x(1), x(2), \ldots, x(N-m+1)]$ in m-dimensional space can be constructed such that $x(i) = [u(i), u(i+1), \ldots, u(i+m-1)]$. Using $x(i)$, an additional quantity, C_i^m, can be calculated:

$$C_i^m(r) = \frac{\text{number of x(j) such that } |x(i) - x(j)| < r}{N - m + 1}$$

where r is an arbitrary tolerance. This can be used to define

$$\Phi^m(r) = \frac{1}{N-m+1} \sum_{i=1}^{N-m+1} \log(C_i^m(r)) \qquad (2)$$

such that

$$\text{ApEn} = \Phi^m(r) - \Phi^{m+1}(r) \qquad (3)$$

We calculated ApEn with an m of 2, and r equal to 0.2*(standard deviation of data), as previous research has shown that this choice in parameters yields statistically reliable and reproducible results (Pincus, 1995, Pincus and Goldberger, 1994). ApEn was calculated separately for three trials for each patient in the delta, theta, alpha and beta (13-35 Hz) frequency bands for each channel. These values were then averaged over the trials and over the channels to obtain a single descriptor as a feature in the classification scheme.

Permutation Entropy

In contrast to ApEn, permutation entropy makes use of the symbolic transform, such that the signal is represented by a sequence of discrete symbols, the probability density of which is analysed to obtain the entropy. Symbolization of EEG data is a useful practice because it reduces sensitivity to noise, simplifies computational evaluations, and consequently increases efficiency in quantifying information from a complex dynamical system (Daw *et al.*, 2003). The transformation involves the extraction of sub-vectors of the signal, each composed of voltages at m time points separated by a fixed time delay, τ. Each sub-vector is then assigned a unique symbol, dependent only on the order of the amplitudes, such that there are $m!$ possible symbols. Permutation entropy can then be calculated as,

$$\text{Permutation entropy} = -\sum_{i=1}^{m!} p_i \log(p_i) \qquad (4)$$

where p_i is the probability of occurrence of the i^{th} motif.

Permutation entropy was calculated over ten trials for each channel in the delta, theta, alpha and beta bands separately, using a time delay τ of one sample and an embedding dimension m of 3: Figure 2 provides an illustration of the $3! = 6$ possible symbol representations of sub-vectors. Feature vectors for the classification scheme were obtained in a similar manner to those in the ApEn analysis.

3.3 Power in alpha and delta frequency bands

Some studies have shown that differences in power spectra exist between comatose patients and healthy controls, as well as between UWS and MCS patients (Lehmann *et al.*, 1987, Blume *et al.*, 2015, Stender *et al.*, 2015). In particular, these studies have indicated that comatose patients exhibit reduced power in the alpha band and increased power in the delta band, with a more severe difference presented in the UWS than the MCS. We verify these results by establishing how accurately power in these bands differentiate patients in the UWS and MCS, and furthermore we determine the effectiveness of using spectral power in these frequency bands to prognosticate coma.

To do so, relative power values were obtained in the alpha and delta bands by computing the power in these bands as a fraction of the power across 1-50Hz, which were then used as features in the classification scheme.

A multitaper method was employed to overcome some of the limitations of conventional Fourier analysis. In principle, to describe a system in the frequency domain, an output sample of infinite length is needed. Moreover, infinitely many realisations of this output is needed to capture stochastic properties, which in most scenarios is not possible. Typically, the output is only observed as a single realisation with finite length, which often results in spectral estimates that are biased and exhibit high error variance (Babadi and Brown, 2014).

To remedy this, several periodograms were obtained by multiplying the EEG signal with Slepian sequences, a family of mutually orthogonal tapers (windows) which additionally have optimal time-frequency concentration properties (Van De Ville

et al., 2002). These periodograms (each one obtained using a different Slepian sequence as a window) were then averaged to produce the multitaper power spectral density estimate. Slepian sequences, $\hat{g}_n$, are defined as the eigenvectors of,

$$\sum_{n=0}^{N-1} \frac{\sin(2\pi W(m-n))}{\pi(m-n)} \hat{g}_n = \lambda \hat{g}_n \qquad (5)$$

where N is the number of time samples of EEG data for one channel, and W is a half-bandwidth that defines a small frequency band centred around f. Here, we chose W of 0.002, and made use of the first 7 Slepian sequences based on the value of the corresponding eigenvalues.

3.4 Connectivity

Some research has been done into comparing the brain connectivity of UWS and MCS through indices like coherence, the imaginary part of coherence, weighted symbolic mutual information and symbolic transfer entropy, all of which are further explored in this study (Lehembre *et al.*, 2012, King *et al.*, 2013, Lee *et al.*, 2015). These indices provide insight into the degree of integration and connection of networks in the brain by assessing connectivity between electrodes.

Coherence

Coherence quantifies the degree of coupling of frequency spectra between two electrodes, and can be calculated for a frequency f as,

$$C_{xy}(f) = \frac{|G_{xy}(f)|^2}{G_{xx}(f)G_{yy}(f)} \qquad (6)$$

where $G_{xy}(f)$ is the cross-spectral density of x and y, where x and y are time-series of voltages recorded at different electrodes, and $G_{xx}(f)$ and $G_{yy}(f)$ are the auto spectral density of x and y respectively.

Coherence is a well-studied measure of connectivity that has been applied in numerous EEG studies, but has the significant disadvantage of being contaminated by volume conduction, which is the transmission of electrical signals from a primary source through brain tissue (Nunez *et al.*, 1997). To overcome this issue, and thereby provide a more accurate reflection of brain interactions, one approach is to consider only the imaginary part of coherence since volume conduction only affects the real part of coherency.

Magnitude-squared coherence and the imaginary part of coherence were calculated for each patient for each pair of electrodes in the delta, theta, alpha and beta frequency bands and averaged over three trials. The median value of coherence for each electrode was then determined, and the mean of these median values used as a feature in the classification scheme.

Weighted Symbolic Mutual Information

The weighted symbolic mutual information (wSMI) is based on principles of permutation entropy applied to the quantification of global information sharing (King *et al.*, 2013). The method assesses the joint occurrences of symbolic or qualitative fluctuations in the signal, thus robustly detecting non-directional nonlinear coupling. To account for spurious correlations produced by artifacts (such as those from volume conduction), wSMI disregards trivial conjunctions of symbols across two signals, corresponding to conjunctions of identical symbols, as well as conjunctions of opposite symbols. This is achieved by attributing a zero weight to symbol pairs indicated on the joint probability matrix illustrated in Figure 3. The reasoning behind the zero-weighting is that conjunctions of identical symbols may be elicited by a common source, and conjunctions of opposite symbols may reflect opposite sides of a common electric dipole.

To calculate wSMI, the EEG data is symbolically transformed as described for the calculation of permutation entropy: data points are divided into sub-vectors of dimension m, with each element in the sub-vector separated by a fixed time delay, τ, similarly to the embedding performed for the calculation of permutation entropy.

wSMI can then be determined as follows,

$$\text{wSMI} = \frac{1}{\log(m!)} \sum_{x \in X} \sum_{y \in Y} w(x,y) p(x,y) \log \frac{p(x,y)}{p(x)p(y)} \quad (7)$$

where x and y are motifs present in signals X and Y respectively, $p(x,y)$ is the joint probability of co-occurence of x and y, $p(x)$ is the probability of occurrence of x, similarly $p(y)$ is the probability of occurrence of y, and $w(x,y)$ is the weight with value 0 or 1. wSMI was determined in the delta, theta, alpha and beta frequency bands with m of 3 and τ of 4, 8 and 32 time samples. Figure 3 shows the probability matrix used to calculate wSMI for a m of 3, and illustrates the $3! = 6$ possible symbol representations of sub-vectors.

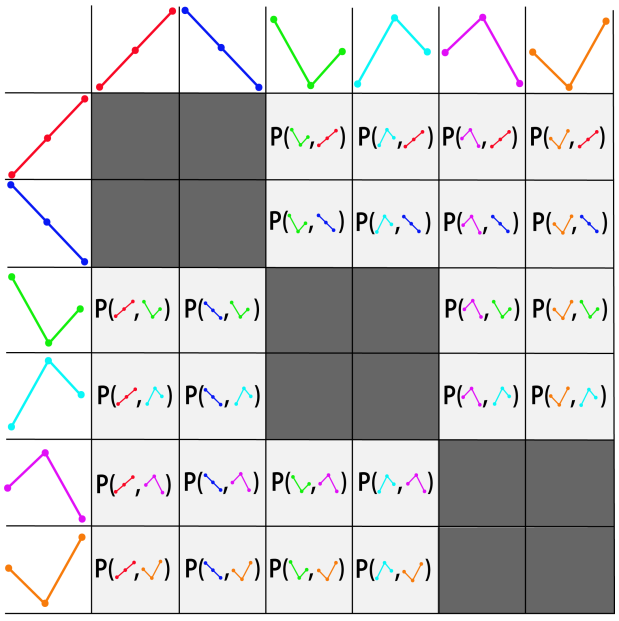

Fig. 3. The joint probability matrix for a symbol transformation with $m = 3$. Dark grey blocks are zero-weighted ($w = 0$) and do not contribute to the wSMI.

Symbolic Transfer Entropy

Transfer entropy (TE) quantifies the directional transfer of information by assessing the uncertainty of the current value of voltage at one electrode position Y knowing past voltages at another position X compared to the uncertainty in the voltage at Y only knowing past voltages at Y. TE is based on Granger Causality, a linear regression model that quantifies the casual interaction between a source signal X and target signal Y: X is said to Granger-cause Y if the inclusion of the past of X improves the prediction of Y (Barnett *et al.*, 2009). TE thus differs from Granger Causality in that it is framed in terms of resolution of uncertainty, not in terms of prediction. However, it has been shown that TE is equivalent to Granger Causality under Gaussian assumptions (Barnett *et al.*, 2009). Granger Causality is known to produce spurious results due to its linearity, sensitivity to noise, and sensitivity to band-pass filtering. TE is a robust, nonlinear approach that was consequently introduced to address these limitations (Lee *et al.*, 2015).

TE offers a model-free estimation of the direction and strength of connectivity between two signals, X and Y, and can be defined as the measure of mutual information between the past of X, (X_P), and the future of Y, (Y_F), when the past of Y, (Y_P) is already known.

Mathematically,

$$\text{TE}_{X \to Y} = \sum P(Y_F, Y_P, X_P) \log \left[\frac{P(Y_F | Y_P, X_P)}{P(Y_F, Y_P)} \right] \quad (8)$$

However, TE can be quite complex to determine because of the difficulty in estimating probability density functions from finite, irregular data. Moreover, to do so, data is quantised into equally-spaced bins, and it has been shown that TE estimates are dependent on this arbitrary choice in bin-size. To overcome this, we investigate symbolic transfer entropy, which quantifies TE of symbolically transformed data without the need for binning or advanced estimators of the probability density function.

The EEG data is symbolically transformed as described previously with a embedding dimension of $m = 3$ and time delay $\tau = 1$, and TE calculated for each patient in the delta, theta, alpha and beta frequency bands. Feature vectors were obtained by

averaging TE over all electrodes and over 10 trials of data.

3.5 Complex Network Analysis

Measures of connectivity can be employed in complex network analysis which aims to represent complex systems as networks and extract meaningful information from the topologies of these networks. Complex network analysis may be a particularly insightful tool because it allows the exploration of structural-functional connectivity relationships by defining functional connections with respect to the spatial map of the brain. In EEG analyses, networks can be constructed by considering the electrode positions as nodes and the links between nodes as functional connections, as quantified by measures like those discussed previously. This study makes use of non-directional binary links such that a link is either present or absent depending on a threshold value of the connectivity measure. Such a network that incorporates EEG results as described here is visualised in Figure 4.

The topology of these networks can be assessed and compared through the graph-theoretical measures, like the clustering coefficient and characteristic path length. The clustering coefficient of a network can be computed by examining triplets, which are defined as three nodes with at least two links. Specifically, the clustering coefficient is defined as the number of closed triplets (groups of three nodes which are interconnected) divided by the total number of triplets. The clustering coefficient is thus a micro-scale measure that provides an indication of clustered connectivity around individual nodes, which in turn is indicative of segregated neural processing. Conversely, characteristic path length is defined as the average number of steps along the shortest paths for all possible pairs of nodes, where each path represents a potential route of information flow between two brain regions.

The average clustering coefficient and characteristic path length were both examined in this study, with links between nodes determined by thresholding values for coherence between electrodes. Coherence in the delta, theta, alpha and beta ranges were thresholded at varying values between 0.8 and 0.99, such that a link is said to exist between two nodes if the coherence between the two corresponding electrodes is above the threshold.

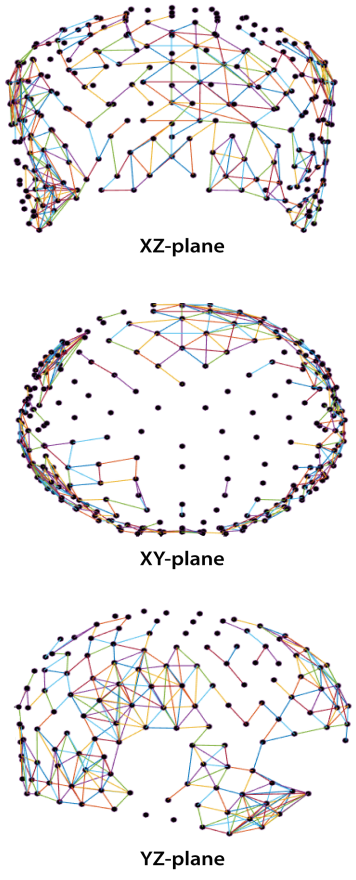

Fig. 4. A visualisation in the XZ- , XY- and YZ- planes of complex network analysis applied to EEG: this is an example of the network obtained for one patient when thresholding coherence in the beta range at 0.94. The nodes are represented by electrodes and binary non-directional links between two electrodes indicate a coherence of greater than 0.94 between those electrodes.

4 Results

We investigated the power of various EEG biomarkers in discriminating UWS and MCS patients as well as in predicting coma outcome, and found that many of these measures performed significantly better than randomly permuted feature vectors.

4.1 Indexing consciousness

We represented EEG signals as complex network graphs by thresholding coherence in the beta range, and found that both the characteristic path length and the clustering coefficient of these graphs successfully classified patients into UWS/MCS. The characteristic path lengths of complex networks obtained by thresholding beta coherence yielded high classification accuracy using thresholds between 0.9 and 0.96, with a threshold of 0.96 proving to be optimal (AUC = 70% $\pm$ 3%, q < 0.0001). However, the most promising results were obtained using characteristic path lengths calculated from alpha coherence thresholded at 0.95 (AUC = 78% $\pm$ 3%, q < 0.0001).

Also investigated in the complex network analysis, the clustering coefficient calculated from beta coherence thresholded at 0.99 best discriminated UWS/MCS patients (AUC = 74 % $\pm$ 2%, q < 0.0001), but significant results were also obtained using thresholds of 0.85, 0.94 and 0.98.

Both permutation entropy and ApEn also performed well at classifying UWS/MCS patients: significant results were achieved using permutation entropy in the delta band (AUC = 67% $\pm$ 3%, q < 0.0001), as well as ApEn in the delta, theta and alpha bands, with ApEn in the alpha band (AUC = 73% $\pm$ 6%, q < 0.0001) and the theta band (AUC = 71% $\pm$ 3%, q < 0.0001) performing most effectively.

Power in the alpha band performed similarly at indexing consciousness (AUC = 70% $\pm$ 3%, q < 0.0001), although power in the delta band held no significant discriminatory power, in contrast to the findings of Lehembre *et al.* (2012).

Measures of connectivity did not perform as successfully as other measures at discriminating UWS/MCS patients. Of all the connectivity measures studied, only theta coherence (AUC = 60% $\pm$ 4%, q < 0.001) and beta coherence (AUC = 62% $\pm$ 4%, q < 0.0001) achieved significant results.

Only the measures described above separated UWS/MCS patients proficiently, meaning that TE, wSMI and measures obtained in the microstate analyses exhibited no significant discriminatory power. It is interesting that wSMI did not perform significantly at classifying UWS/MCS patients in any of the frequency bands or for any of the time delays studied, as this is in contrast to the findings of Sitt *et al.* and King *et al.* (King *et al.*, 2013, Sitt *et al.*, 2014). This may potentially indicate constraints on the use of wSMI in indexing consciousness.

4.2 Predicting outcome

Many more measures performed better than expected by chance at predicting outcome than at discriminating UWS/MCS patients, and additionally greater classification sensitivity and specificity was obtained when predicting outcome.

It was found that the clustering coefficient, calculated from beta coherence thresholded at 0.94, best classified patients into positive and negative outcome (AUC = 88% $\pm$ 3%, q < 0.0001). However, results obtained using thresholds of 0.85, 0.93-0.96, 0.98 and 0.99 were also significant. Furthermore, meaningful results were achieved using characteristic path lengths

calculated from beta coherence thresholded at 0.85-0.90, 96 and 97, with a threshold of 0.86 yielding the best results (AUC = 75 % 3, $q < 0.0001$).

ApEn in the alpha band efficiently predicted outcome (AUC = 68% $\pm$ 6%, q <0.001), and ApEn in the gamma band also performed significantly better than expected by chance. Permutation entropy did not perform as well as ApEn: only permutation entropy in the delta band was proficient at classifying patients by outcome (AUC = 64% $\pm$ 4%, $q < 0.01$).

Power in the alpha band also exhibited predictive power (AUC = 68% $\pm$ 5%, $q < 0.0001$), but once again power in the delta band did not achieve significant results.

In contrast to the investigation on indexing consciousness, all measures of connectivity were successful in predicting outcome. Coherence in the beta band yielded high classification accuracy (AUC = 70% $\pm$ 3%, $q < 0.0001$), and delta and alpha coherence were also successful. Interestingly, only the imaginary part of coherence in the delta band achieved significant results (AUC = 66% $\pm$ 4%, $q < 0.0001$) and did not offer an advantage to magnitude-squared coherence as a classifier. This may indicate the potential importance of information contained in the real part of coherence.

The other measures of connectivity studied, TE and wSMI, both also effectively predicted patient outcome. We found that TE with the parameters chosen here was successful in the delta band at predicting outcome (AUC = 66% $\pm$ 5%, q <0.001), and wSMI in the delta band with $\tau = 8$ exhibited notable prognostic power (AUC = 66 % $\pm$ 5 %, $q <$ 0.001).

In all frequency bands, we found that the durations of microstates afforded accurate classification with respect to outcome, with the durations of microstates in the theta and the 2-20Hz frequency bands performing the best (AUC = 78% $\pm$ 3%, $q < 0.0001$). The similarity of these results can likely be attributed to the equivalence of the microstates obtained in these two frequency bands, as shown in Figure 1. The frequency of microstates offered no significant predictive value, whereas the percentage of time spent in each microstate in the delta band performed only weakly in classifying outcome (AUC = 64% $\pm$ 6%, $q < 0.01$).

4.3 Automatic classification

The 3 best-performing features at predicting outcome were combined in a single classification scheme, with the intent of developing an accurate, automatic tool for coma outcome prediction. To this effect, we included as features the duration of microstates belonging to class C, characteristic path length calculated using beta coherence thresholded at 0.86, and lastly the clustering coefficient of EEG network graphs produced by thresholding beta coherence at 0.94.

The automatic classification scheme proved to be an effective and accurate means of predicting outcome (AUC = 95% $\pm$ 2%, $q < 0.0001$), with possible application in clinical practice.

5 Discussion

We investigated several descriptive measures extracted from EEG signals of comatose patients with respect to prognostic power, and showed that the clustering coefficient of EEG signals represented as complex network graphs performed best at classifying patients into positive and negative outcome. Additionally, several features performed significantly better than random permutations at predicting outcome and/or at discriminating UWS from MCS, although with less specificity and sensitivity than the clustering coefficient, as indicated by lower AUC scores.

Most measures performed significantly better at

predicting outcome of coma than at discriminating between UWS and MCS patients, indicating perhaps that the link between diagnosis and prognosis is not as compelling as originally thought, or perhaps that some patients had been erroneously classified, considering that in clinical practice misdiagnoses occur in up to 43% of cases, especially when an inappropriate behavioural scale is used (Schnakers *et al.*, 2009). Additionally, these strictly-defined categories do not take into account that UWS patients may actually be minimally or even fully conscious (van Erp *et al.*, 2015b). It is also interesting to note that this study obtained contrasting results to other studies on the diagnostic value of wSMI as well as power in the delta band, potentially indicating that these measures are dependent on the type of EEG data investigated. For example, this study makes use of resting-state data, whereas King *et al.* analysed data of patients presented with an auditory paradigm.

While effective and accurate, the methods and measures studied here have not performed sufficiently well to replace current practice for prognosticating coma on an individual basis. However, the automatic classification scheme is simple and cost-effective to implement and may indeed provide supplemental information to better inform medical practitioners when assessing prognosis. Moreover, the results of this study may not only be useful in clinical practice, but also in better understanding the nature of consciousness and the roots of disorders of consciousness.

Recent theories attribute disorders of consciousness to the disconnection of different cortical networks, rather than the dysfunction of a single area of the brain (Ovadia-Caro *et al.*, 2012, Vanhaudenhuyse *et al.*, 2010). For this reason, it may be important to investigate the structure of neural networks underlying consciousness and its interconnectedness through measures of functional connectivity, like those explored in this study. It is possible that disorders of consciousness stem from a functional isolation within the cerebral cortex, due to a derangement of neural networks and a consequent decrease in complexity and connectivity. The measures of connectivity, entropy and graph-theoretical statistics investigated here directly assess the degree of functional isolation through the investigation of the interconnectedness of subdivisions within the neural networks, as well as the complexity of these neural networks though the quantification of the unpredictability of its outputs. While the measures studied here do support this proposed theory of consciousness to some extent, it is entirely possible that other measures may better reflect true brain interactions, and consequently be more successful at interrogating differences between positive and negative outcome patients. It is thus necessary to continue to propose EEG methods to accurately reveal interactions between different cortical networks, and compare the results to those from other brain imagining methods, such as fMRI. These new methods of analysis may then firstly contribute additional evidence to the leading theory or otherwise, and secondly prove to be more useful in prognosticating coma than the methods studied here.

6 Conclusion

A multidisciplinary approach to neuroscience that combines mathematics, statistics and computer science has the potential to reveal insights about the state and function of the brain of comatose patients. We have shown here that several mathematically-determined biomarkers perform significantly better than expected by chance at predicting outcome of coma, with the most promising results obtained through the analysis of EEG signals represented as complex network graphs. If the nodes are represented by electrodes, and non-directional binary links determined by thresholding coherence in the

beta range at 0.94, then the clustering coefficient of the resulting network performs most successfully at classifying patients into positive and negative outcome (AUC = 88% ± 3%, $q < 0.0001$). The path length of the network determined by thresholding coherence in the alpha range most successfully discriminated between UWS and MCS patients (AUC = 78%, $q < 0.0001$), which is useful considering that in clinical practice diagnosis plays a key role in prognosis.

Lastly, the 3 measures that performed most successfully at predicting outcome were combined into a single classification scheme. This resulted in an effective and automatic method of predicting coma outcome (AUC= 95% ± 2%, $q < 0.0001$). While this may still not be suitable for prognostication of individuals, it may indeed serve to better inform medical practitioners when assessing prognosis.

Accurate and reliable prognosis of coma is important for therapeutic, ethical and economic reasons, and the results of this study may contribute to achieving this goal by supplementing information considered by medical practitioners when examining patients.

Acknowledgements

Computations were performed using facilities provided by the University of Cape Town's ICTS High Performance Computing team: http://hpc.uct.ac.za. Many thanks to Dr Jonathan Shock for his input, suggestions and advice.

References

Babadi, B. and Brown, E. N. (2014). A review of multitaper spectral analysis. *Biomedical Engineering, IEEE Transactions on*, **61**(5), 1555–1564.

Barnett, L., Barrett, A. B., and Seth, A. K. (2009). Granger causality and transfer entropy are equivalent for gaussian variables. *Physical review letters*, **103**(23), 238701.

Blume, C., del Giudice, R., Wislowska, M., Lechinger, J., and Schabus, M. (2015). Across the consciousness continuumâĽ"from unresponsive wakefulness to sleep. *Frontiers in human neuroscience*, **9**.

Bradley, W. G. (2004). *Neurology in clinical practice: principles of diagnosis and management*, volume 1. Taylor & Francis.

Brodbeck, V., Kuhn, A., von Wegner, F., Morzelewski, A., Tagliazucchi, E., Borisov, S., Michel, C. M., and Laufs, H. (2012). Eeg microstates of wakefulness and nrem sleep. *Neuroimage*, **62**(3), 2129–2139.

Bruhn, J., Röpcke, H., and Hoeft, A. (2000). Approximate entropy as an electroencephalographic measure of anesthetic drug effect during desflurane anesthesia. *Anesthesiology*, **92**(3), 715–726.

Daw, C. S., Finney, C. E. A., and Tracy, E. R. (2003). A review of symbolic analysis of experimental data. *Review of Scientific Instruments*, **74**(2), 915–930.

Giacino, J. T. (2004). The vegetative and minimally conscious states: consensus-based criteria for establishing diagnosis and prognosis. *NeuroRehabilitation-An Interdisciplinary Journal*, **19**(4), 293–298.

Giacino, J. T., Ashwal, S., Childs, N., Cranford, R., Jennett, B., Katz, D. I., Kelly, J. P., Rosenberg, J. H., Whyte, J., Zafonte, R., *et al.* (2002). The minimally conscious state definition and diagnostic criteria. *Neurology*, **58**(3), 349–353.

Gosseries, O., Schnakers, C., Ledoux, D., Vanhaudenhuyse, A., Bruno, M.-A., Demertzi, A., Noirhomme, Q., Lehembre, R., Damas, P., Goldman, S., *et al.* (2011). Automated eeg entropy measurements in coma, vegetative state/unresponsive wakefulness syndrome and minimally conscious state. *Functional neurology*.

Kannathal, N., Choo, M. L., Acharya, U. R., and Sadasivan, P. (2005). Entropies for detection of epilepsy in eeg. *Computer methods and programs in biomedicine*, **80**(3), 187–194.

King, J.-R., Sitt, J. D., Faugeras, F., Rohaut, B., El Karoui, I., Cohen, L., Naccache, L., and Dehaene, S. (2013). Information sharing in the brain indexes consciousness in noncommunicative patients. *Current Biology*, **23**(19), 1914–1919.

Koenig, T. and Melie-García, L. (2010). A method to determine the presence of averaged event-related fields using randomization tests. *Brain topography*, **23**(3), 233–242.

Kuhn, A., Brodbeck, V., Tagliazucchi, E., Morzelewski, A., von Wegner, F., and Laufs, H. (2014). Narcoleptic patients show fragmented eeg-microstructure during early nrem sleep. *Brain topography*, pages 1–17.

Laureys, S., Goldman, S., Phillips, C., Van Bogaert, P., Aerts, J., Luxen, A., Franck, G., and Maquet, P. (1999). Impaired effective cortical connectivity in vegetative state: preliminary investigation using pet. *Neuroimage*, **9**(4), 377–382.

Laureys, S., Faymonville, M.-E., Luxen, A., Lamy, M., Franck, G., and Maquet, P. (2000). Restoration of thalamocortical connectivity after recovery from persistent vegetative state. *The Lancet*, **355**(9217), 1790–1791.

Laureys, S., Celesia, G. G., Cohadon, F., Lavrijsen, J., León-Carrión, J., Sannita, W. G., Sazbon, L., Schmutzhard, E., von Wild, K. R., Zeman, A., *et al.* (2010). Unresponsive wakefulness syndrome: a new name for the vegetative state or apallic syndrome. *BMC medicine*, **8**(1), 68.

Lee, U., Blain-Moraes, S., and Mashour, G. A. (2015). Assessing levels of consciousness with symbolic analysis. *Philosophical Transactions of the Royal Society of London A: Mathematical, Physical and Engineering Sciences*, **373**(2034), 20140117.

Lehembre, R., Bruno, M.-A., Vanhaudenhuyse, A., Chatelle, C., Cologan, V., Leclercq, Y., Soddu, A., Macq, B., Laureys, S., and Noirhomme, Q. (2012). Resting-state eeg study of comatose patients: a connectivity and frequency

analysis to find differences between vegetative and minimally conscious states. *Functional neurology*, **27**(1).

Lehmann, D., Ozaki, H., and Pal, I. (1987). Eeg alpha map series: brain micro-states by space-oriented adaptive segmentation. *Electroencephalography and clinical neurophysiology*, **67**(3), 271–288.

Lehmann, D., Strik, W., Henggeler, B., Koenig, T., and Koukkou, M. (1998). Brain electric microstates and momentary conscious mind states as building blocks of spontaneous thinking: I. visual imagery and abstract thoughts. *International Journal of Psychophysiology*, **29**(1), 1–11.

Lehmann, D., Faber, P. L., Galderisi, S., Herrmann, W. M., Kinoshita, T., Koukkou, M., Mucci, A., Pascual-Marqui, R. D., Saito, N., Wackermann, J., *et al.* (2005). Eeg microstate duration and syntax in acute, medication-naive, first-episode schizophrenia: a multi-center study. *Psychiatry Research: Neuroimaging*, **138**(2), 141–156.

Lopez-Rolon, A., Bender, A., *et al.* (2015). Hypoxia and outcome prediction in early-stage coma (project hope): an observational prospective cohort study. *BMC neurology*, **15**(1), 82.

Mason, S. J. and Graham, N. (2002). Areas beneath the relative operating characteristics (roc) and relative operating levels (rol) curves: Statistical significance and interpretation. *Quarterly Journal of the Royal Meteorological Society*, **128**(584), 2145–2166.

Michel, C. M. (2009). *Electrical neuroimaging*. Cambridge University Press.

Murray, M. M., Brunet, D., and Michel, C. M. (2008). Topographic erp analyses: a step-by-step tutorial review. *Brain topography*, **20**(4), 249–264.

Nunez, P. L., Srinivasan, R., Westdorp, A. F., Wijesinghe, R. S., Tucker, D. M., Silberstein, R. B., and Cadusch, P. J. (1997). Eeg coherency: I: statistics, reference electrode, volume conduction, laplacians, cortical imaging, and interpretation at multiple scales. *Electroencephalography and clinical neurophysiology*, **103**(5), 499–515.

Ovadia-Caro, S., Nir, Y., Soddu, A., Ramot, M., Hesselmann, G., Vanhaudenhuyse, A., Dinstein, I., Tshibanda, J.-F. L., Boly, M., Harel, M., *et al.* (2012). Reduction in inter-hemispheric connectivity in disorders of consciousness.

Pascual-Marqui, R. D., Michel, C. M., and Lehmann, D. (1995). Segmentation of brain electrical activity into microstates: model estimation and validation. *Biomedical Engineering, IEEE Transactions on*, **42**(7), 658–665.

Pincus, S. (1995). Approximate entropy (apen) as a complexity measure. *Chaos: An Interdisciplinary Journal of Nonlinear Science*, **5**(1), 110–117.

Pincus, S. M. and Goldberger, A. L. (1994). Physiological time-series analysis: what does regularity quantify? *American Journal of Physiology-Heart and Circulatory Physiology*, **266**(4), H1643–H1656.

Plum, F. and Posner, J. B. (1982). *The diagnosis of stupor and coma*. Oxford University Press.

Sarà, M., Pistoia, F., Pasqualetti, P., Sebastiano, F., Onorati, P., and Rossini, P. M. (2011). Functional isolation within the cerebral cortex in the vegetative state a nonlinear method to predict clinical outcomes. *Neurorehabilitation and neural repair*, **25**(1), 35–42.

Schlegel, F., Lehmann, D., Faber, P. L., Milz, P., and Gianotti, L. R. (2012). Eeg microstates during resting represent personality differences. *Brain topography*, **25**(1), 20–26.

Schnakers, C., Vanhaudenhuyse, A., Giacino, J., Ventura, M., Boly, M., Majerus, S., Moonen, G., and Laureys, S. (2009). Diagnostic accuracy of the vegetative and minimally conscious state: clinical consensus versus standardized neurobehavioral assessment. *BMC neurology*, **9**(1), 35.

Sitt, J. D., King, J.-R., El Karoui, I., Rohaut, B., Faugeras, F., Gramfort, A., Cohen, L., Sigman, M., Dehaene, S., and Naccache, L. (2014). Large scale screening of neural signatures of consciousness in patients in a vegetative or minimally conscious state. *Brain*, **137**(8), 2258–2270.

Stender, J., Gjedde, A., and Laureys, S. (2015). Detection of consciousness in the severely injured brain. In *Annual Update in Intensive Care and Emergency Medicine 2015*, pages 495–506. Springer.

Van De Ville, D., Philips, W., and Lemahieu, I. (2002). On the n-dimensional extension of the discrete prolate spheroidal window. *Signal Processing Letters, IEEE*, **9**(3), 89–91.

van Erp, W. S., Lavrijsen, J. C., Vos, P. E., Bor, H., Laureys, S., and Koopmans, R. T. (2015a). The vegetative state: Prevalence, misdiagnosis, and treatment limitations. *Journal of the American Medical Directors Association*, **16**(1), 85–e9.

van Erp, W. S., Lavrijsen, J. C., Vos, P. E., Bor, H., Laureys, S., and Koopmans, R. T. (2015b). The vegetative state: Prevalence, misdiagnosis, and treatment limitations. *Journal of the American Medical Directors Association*, **16**(1), 85–e9.

Vanhaudenhuyse, A., Noirhomme, Q., Tshibanda, L. J.-F., Bruno, M.-A., Boveroux, P., Schnakers, C., Soddu, A., Perlbarg, V., Ledoux, D., Brichant, J.-F., *et al.* (2010). Default network connectivity reflects the level of consciousness in non-communicative brain-damaged patients. *Brain*, **133**(1), 161–171.